American Journal of Energy and Power Engineering
2015; 2(6): 79-91
Published online December 17, 2015 (http://www.aascit.org/journal/ajepe)
ISSN: 2375-3897

AASCIT American Association for Science and Technology

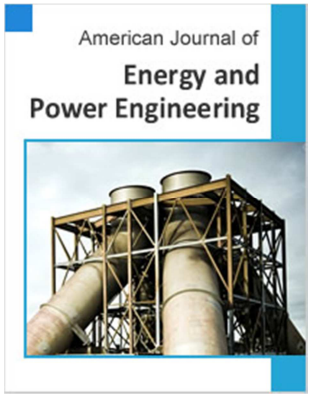

Keywords
Batteries,
Hydrogen,
Solid-Gas Method,
Cyclic Voltammetry,
Electrochemical Impedance Spectroscopy,
Hydrogen Diffusion Coefficient

Received: August 23, 2015
Revised: October 19, 2015
Accepted: October 21, 2015

Study of Structural, Thermodynamic and Electrochemical Properties of $MmNi_{3.55}Mn_{0.4}Al_{0.3}Co_{0.75-x}Fe_x$ (x = 0 and 0.75) Compounds

A. Ben Fradj[1], M. Ben Moussa[1, 2, 3, *], M. Abdellaoui[1], J. Lamloumi[2]

[1]Institute National of Research and Physico-Chemical Analysis, Laboratory of Materials, Ministry of Research, Sidi Thabet, Tunisia
[2]Superior School of Sciences and Technology of Tunis, Laboratory of Materials and Processes, Department of Physics, University of Tunis, Tunis, Tunisia
[3]College of Applied Sciences, Department of Physics, Umm Al Qura University, Makkah, Saudi Arabia

Email address
phmoussa@yahoo.fr (M. Ben. Moussa)

Citation
A. Ben Fradj, M. Ben Moussa, M. Abdellaoui, J. Lamloumi. Study of Structural, Thermodynamic and Electrochemical Properties of $MmNi_{3.55}Mn_{0.4}Al_{0.3}Co_{0.75-x}Fe_x$ (x = 0 and 0.75) Compounds. *American Journal of Energy and Power Engineering*. Vol. 2, No. 6, 2015, pp. 79-91.

Abstract
The structural, thermodynamic and electrochemical properties of the $MmNi_{3.55}Mn_{0.4}Al_{0.3}Fe_{0.75}$ compound, used as negative electrode of Ni – MH accumulator, are studied and compared to those of $MmNi_{3.55}Mn_{0.4}Al_{0.3}Co_{0.75}$ electrode. The thermodynamic results show that the total substitution of cobalt by iron leads to a decrease solid – gas capacity measured at 25°C from 5.5 H/mol to 3.93 H/ mol for $MmNi_{3.55}Mn_{0.4}Al_{0.3}Co_{0.75}$ and $MmNi_{3.55}Mn_{0.4}Al_{0.3}Fe_{0.75}$ compounds, respectively. The electrochemical discharge capacity for the $MmNi_{3.55}Mn_{0.4}Al_{0.3}Co_{0.75}$ compound reaches its maximum of 270 mAh/g after 12 cycles and then decreases to 200 mAh/g after 25 cycles. However, the electrochemical discharge capacity of the $MmNi_{3.55}Mn_{0.4}Al_{0.3}Fe_{0.75}$ compound reaches its maximum value of 200 mAh/g after 9 cycles and then decreases to 180 mAh/g after 25 cycles. The decrease of the discharge capacity for the two alloys is attributed to the corrosion and deprecipitation of the alloys in the KOH aqueous solution. The value of the hydrogen diffusion coefficient D_H determined by the cyclic voltammetry are equal to 5.85 10^{-10} cm^2 s^{-1} and 3.96 10^{-10} cm^2 s^{-1} for $MmNi_{3.55}Mn_{0.4}Al_{0.3}Co_{0.75}$ and $MmNi_{3.55}Mn_{0.4}Al_{0.3}Fe_{0.75}$ compounds, respectively. The hydrogen diffusion coefficient determined by electrochemical impedance spectroscopy (EIS), corresponding to 10 and 100 % of the charge state are equal to 6.64 10^{-10} cm^2 s^{-1} (α phase) and 1.6 10^{-10} cm^2 s^{-1} (β phase) for the $MmNi_{3.55}Mn_{0.4}Al_{0.3}Co_{0.75}$ alloy. However, for the $MmNi_{3.55}Mn_{0.4}Al_{0.3}Fe_{0.75}$, the hydrogen diffusion coefficient are equal to 7.27 10^{-10} cm^2 s^{-1} (α phase) and 2.51 10^{-10} cm^2 s^{-1} (β phase).

1. Introduction

In recent years, hydrogen may constitute the main energy vector in the future. There is multiple ways of storing hydrogen. An alternative to the use of gaseous pressure tanks is to store hydrogen in metal hydrides. Many of applications of hydrogen storage alloys have been widely used as the negative electrode materials in the nickel – metal hydride (Ni / MH) secondary batteries for their higher energy density, high capacity rate and longer life cycle. The high charge / discharge rate of Ni–MH batteries is gaining increasing attention.

The rapid charging perform ance of the cell is very important for some applications such as mobile phones and electric vehicles.The key to the improvement of the commercial Ni/MH batteries is the improvement of the electrochemical properties of the hydrogen storage alloys including the electrochemical capacity, the life cycle and the high rate of dischargeability.

Most of the negative electrodes of such batteries are made of $LaNi_5$ –type alloy [1, 2]. The behavior of these batteries can be changed when modifying the hydrogen storage alloy to achieve a good performance. The $LaNi_5$ compound, one of the AB_5 – rare type– earth alloys, is the most promising candidate [3, 4]. Nevertheless, it exhibits a high equilibrium pressure of 1.7 bars at room temperature and its electrochemical capacity decreases rapidly when increasing the charge – discharge cycles. This such latte phenomenon was attributed to the oxidation and the formation of the $La(OH)_3$ film at the surface [5]. To decrease the plateau pressure and inhibit the oxidation phenomenon, some works have been carried out to replace the lanthanum by mischmetal (a mixture of different rare earth such as: Ce, Nd and Pr) and a part of nickel atoms with different transition elements such as Mn, Al and Co [6, 7-10].

These commercial AB5 alloys are usually of the type Mm(Ni,Co, Al, Mn)5, containing typically 10 wt% Co. Cobalt is present in the alloys to guarantee the long cycle life of the negative electrode [11]. However, cobalt is also the most expensive metal among the alloying compounds representing 10 % of the weight but 45 % of the total alloy price. Therefore, it is interesting to investigate low-Co or Co-free AB5-type alloys. For this purpose we have studied the influence of the Fe for Co substitution, especially on the life time of the electrode.

In the present work, we have studied the effect of total substitution of Co by Fe on the structural, thermodynamic and electrochemical properties of the MmNi3.55Mn0.4Al0.3Co 0.75 compound. The value of the hydrogen diffusion coefficient DH was determined by the cyclic voltammetry and electrochemical impedance spectroscopy (EIS) have been evaluated the reversibility and the kinetic of the electrochemical reaction of the both alloys.

2. Experimental Detail

The $MmNi_{3.55}Mn_{0.4}Al_{0.3}Fe_{0.75}$ and $MmNi_{3.55}Mn_{0.4}Al_{0.3}Co_{0.75}$ alloys were prepared by UHF induction melting (UHF) of the pure elements followed by an appropriate annealing to ensure a good homogeneity.

They are carefully checked by metallographic examination, electron probe microanalysis (EPMA) and powder X-ray diffraction (XRD) with CuK_α beam.

The pressure-composition -isotherm (P- C - T) was measured using a volumetric (Sievert) method. Each sample was first activated by several hydrating -dehydrating cycles to reduce the grain size and to increase the kinetic.

2.1. Preparation of the M H Electrode and Ni –MH Cell

These ingot alloys were ground mechanically and saved to less than 63μm in a glove box under an argon atmosphere. The "latex" technology has been used for the electrode preparation. Ninety percent of the alloy powder was mixed with 5% of black carbon (to obtain a good conductivity) and5% of polytetrafluoroethylen (PTFE). Two pieces of 0.5 $cm^2$of this latex have been pressed on each side of a nickel grid to prevent the electrode platform breaking into pieces during the charge–discharge cycling [12]. This assembly forms the negative electrode of Ni–MH battery. The counter electrode was formed by the Ni ox hydroxide$Ni(OH)_2$, whereas the reference electrode was the Hg/HgO 1MKOH electrode. The electrolyte was 1M KOH solution, prepared with deionized water.

2.2. Electrochemical Measurements

All the electrochemical measurements were performed at room temperature in a conventional three electrode-open-air cell using a computer- as a controlled response frequency analyser coupled directly to a VMP Biologic potentiostat–galvanostat. The discharge capacity of the electrode was determined by a galvanostatical charging-discharging, respectively, at C/3 and D/6 regime. Every cycle was carried out by charging fully at 120 mA/g for 3 h (this time majored by 50 % due to the efficiency of the charging reaction) and discharging at 60 mAh/g at room temperature. After activating the electrode for 35 cycles, the cyclic voltammetry was applied at scan rates of 10, 20, 30, 40 and 50 μv s^{-1} between −1.1 and −0.5V versus Hg/HgO. Impedance spectroscopy measurements were realized after 13 cycles. The chronoamperommetry was applied after 12 charge-discharge cycles. This method consists of fully charging and discharging the electrode at a constant potential (- 0.6 V versus Hg/HgO).

The electrode was charged to a state of charge (SOC) of 10 % at C/3 regime. After that, a rest of 3 h was applied to the open-circuit potential to get stabilized. The electrochemical impedance spectrum of the electrode was measured by the AC perturbation of ± 5 mV as amplitude and 1 mHz to 50 KHz frequency range for 10 points per decade.

3. Resultats and Discussions

3.1. Structural Properties

EPMA analysis indicates that the composition of these compounds $MmNi_{3.55}Mn_{0.4}Al_{0.3}Fe_{0.75}$ and $MmNi_{3.55}Mn_{0.4}Al_{0.3}Co_{0.75}$ are a single phase and has a homogenous composition in agreement with the nominal one. The diffraction patterns were refined with a Rietveld analysis using the program fullproof represented in Fig. 1 and Fig. 2. The structural characterisation shows that these compounds are indexed in CaCu5 hexagonal crystalline structure (P6/mmm space group). The results of the metallographic

examination, the electron probe microanalysis (EPMA) and the structure characterisation by X-ray diffraction (XRD) of these compounds are given in Table 1. In fact, the lattice parameters and lattice volume increases progressively by the totaly substitution of iron for cobalt, which indicate that the capacities of the as-quenched alloys decrease greatly with the increase of the Fe content [13].

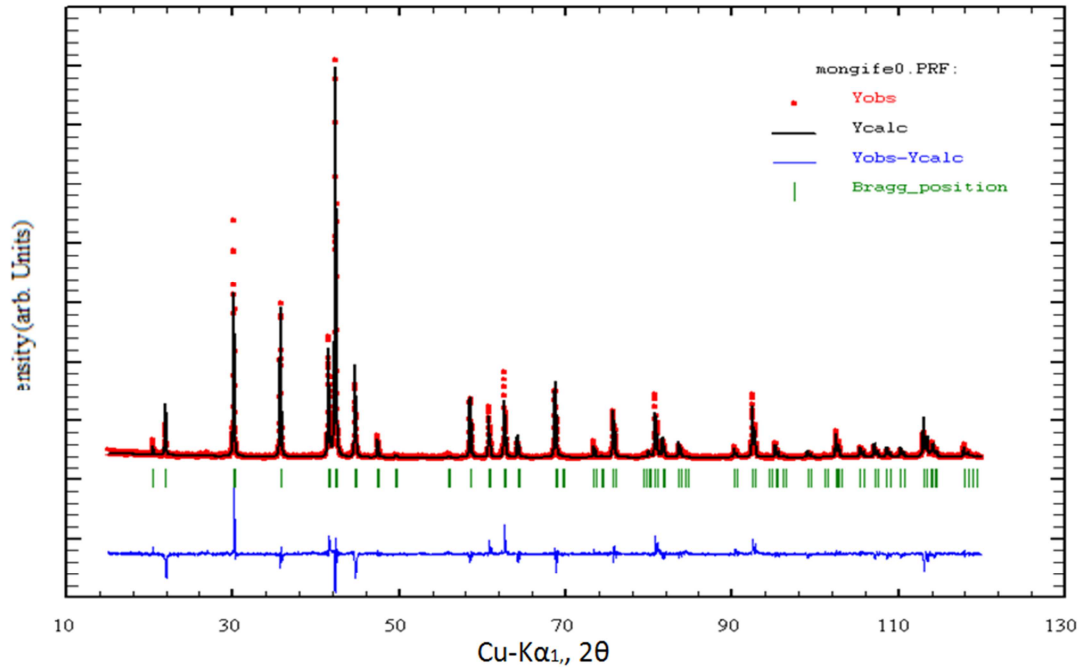

Figure 1. *Refined diffraction pattern of the* $MmNi_{3.55}Mn_{0.4}Al_{0.3}Co_{0.75}$.

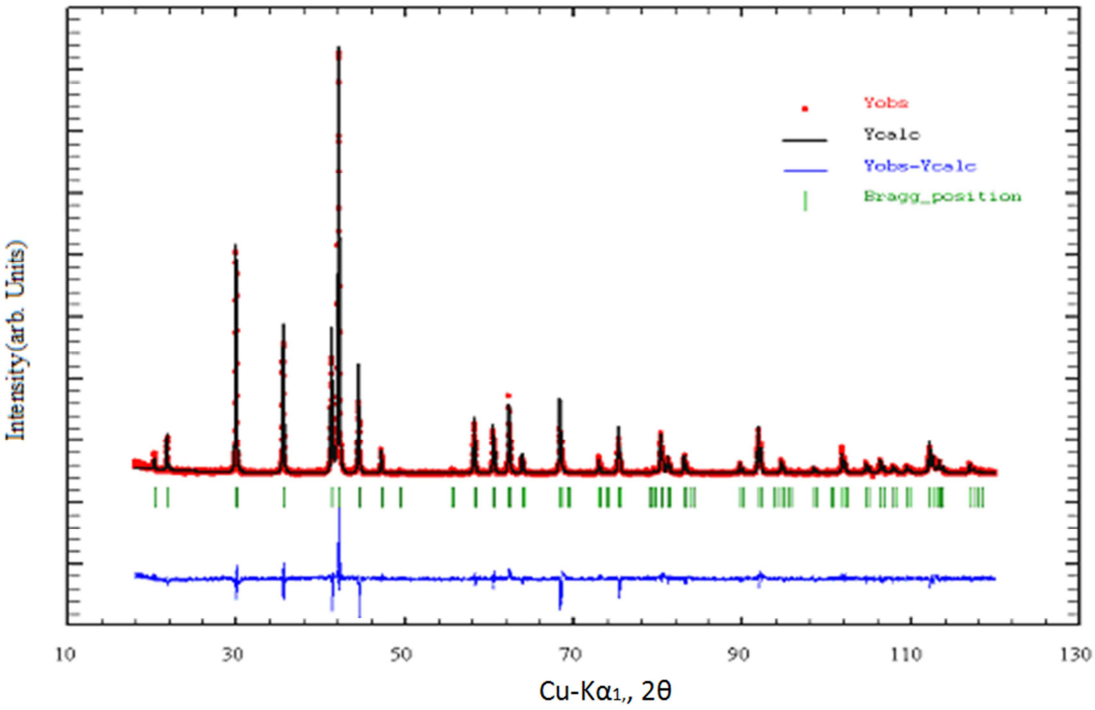

Figure 2. *Refined diffraction pattern of the* $MmNi_{3.55}Mn_{0.4}Al_{0.3}Fe_{0.75}$ *[25].*

Table 1. *Lattice parameters and lattice volume of the substituted compound.*

Compound	a (Å)	c (Å)	V ($Å^3$)
$LaNi_5$	5.012	3.984	86.68
$MmNi_{3.55}Mn_{0.4}Al_{0.3}Co_{0.75}$ [24]	5.019	4.049	88.32
$MmNi_{3.55}Mn_{0.4}Al_{0.3}Fe_{0.75}$ [25, 26]	5.0422	4.067	89.54

3.2. Thermodynamic Properties

The pressure – composition – isotherm (P-C-T) with $MmNi_{3.55}Mn_{0.4}Al_{0.3}Co_{0.75}$ and $MmNi_{3.55}Mn_{0.4}Al_{0.3}Fe_{0.75}$ measured at 25, 40 and 80°C is represented in Fig. 3 and Fig. 4,

where the hydrogen desorption pressure is plotted as a function of an amount of a desorbed hydrogenThese values of solid- gas capacity–and pressure equilibrium at 25, 40 and 80°C are given in Table 2. The solid – gas capacity measured at 25°C from 5.5 H/mol to 3.93 H/ mol for $MmNi_{3.55}Mn_{0.4}Al_{0.3}Co_{0.75}$ and $MmNi_{3.55}Mn_{0.4}Al_{0.3}Fe_{0.75}$ compounds, respectively. The result shows that the substitution of cobalt by iron increases the stability of the compound.

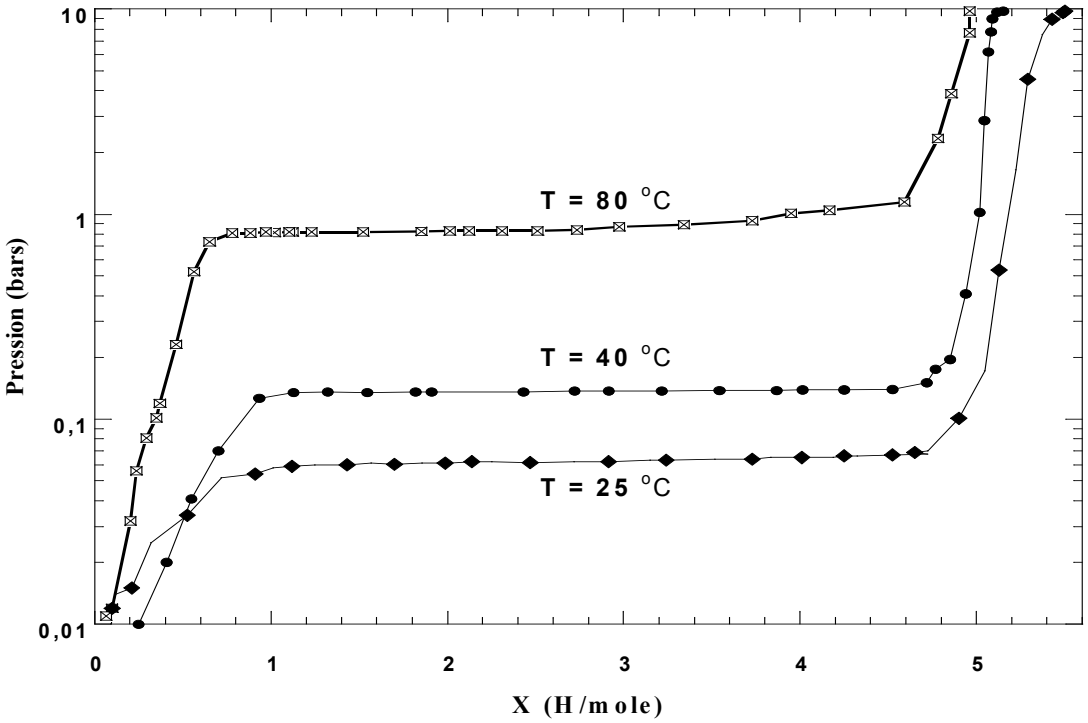

Figure 3. *Isotherm of desorption at 25, 40 and 80 °C of compound* $MmNi_{3.55}Mn_{0.4}Al_{0.3}Co_{0.75}$.

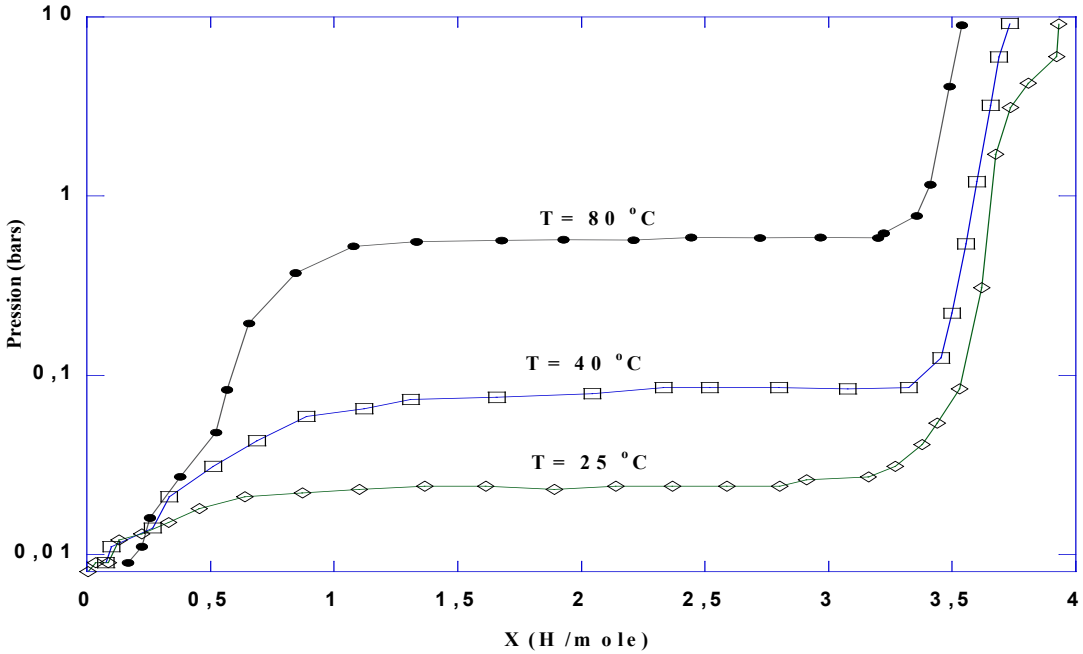

Figure 4. *Isotherm of desorption at 25, 40 and 80 °C of the compound* $MmNi_{3.55}Mn_{0.4}Al_{0.3}Fe_{0.75}$ *[25].*

The pressure equilibrium decrease from 0.065 to 0.024 bars for $MmNi_{3.55}Mn_{0.4}Al_{0.3}Co_{0.75}$ and $MmNi_{3.55}Mn_{0.4}Al_{0.3}Fe_{0.75}$ compounds, respectivelyshows that the substitution of cobalt by iron increases the stability of the compound and can be used as negative electrodes in NiMH batteries or for the hydrogen storage. Referring to the cell volumes listed in Table 1, it can be found that a large cell volume corresponds to a low plateau pressure. It is believed that the expansion of the cell

volume leads to a decrease of the equilibrium pressure.

For both compounds the capacity decreases slightly when the temperature increases. So, for $MmNi_{3.55}Mn_{0.4}Al_{0.3}Co_{0.75}$ compound, the capacity is of 5.5 H / moles at 25°C, and decreases to reach the value of 4.96 H / moles at 80°C. While for the $MmNi_{3.55}Mn_{0.4}Al_{0.3}Fe_{0.75}$ the capacity is of 3.93 H/mole at 25°C, and decreases to reach the value of 3.4 H/mole at 80°C.

The enthalpy and entropy of these hydrides formation, calculated using the equilibrium pressure at 25, 40 and 80°C, are given in Table 3. It is obvious from the data that the absolute value of the alloy enthalpy increases when the cobalt is substituted by iron. This leads to an improved stability of the accordingly prepared hydrides. These results show also that the value of enthalpy formation of the hydride is negative. So, it can be concluded that the reaction of the hydruration is exothermic.

Table 2. *Solid –gas capacity and pressure equilibrium at 25, 40 and 80 °C temperature of $MmNi_{3.55}Mn_{0.4}Al_{0.3}Fe_{0.75}$ and $MmNi_{3.55}Mn_{0.4}Al_{0.3}Co_{0.75}$ compounds.*

	25°C		40°C		80°C	
	P(bar)	Capacity (H/mole)	P(bar)	Capacity (H/mole)	P(bar)	Capacity (H/mole)
$MmNi_{3.55}Mn_{0.4}Al_{0.3}Co_{0.75}$ [25]	0.065	5.50	0.138	5.15	0.82	4.96
$MmNi_{3.55}Mn_{0.4}Al_{0.3}Fe_{0.75}$	0.024	3.93	0.085	3.74	0.582	3.4

Table 3. *The enthalpy and entropy of the formation of these hydrides.*

Compounds	ΔH (Kcal/mole H_2)	ΔS (cal/K/mole H_2)
$MmNi_{3.55}Mn_{0.4}Al_{0.3}Co_{0.75}$	- 9.72	27.09
$MmNi_{3.55}Mn_{0.4}Al_{0.3}Fe_{0.75}$ [26]	- 10.38	28.53

3.3. Electrochemical Properties

3.3.1. Life Time of the Electrode

Fig. 5 shows the variation of the discharge capacity of the $MmNi_{3.55}Mn_{0.4}Al_{0.3}Fe_{0.75}$ and the $MmNi_{3.55}Mn_{0.4}Al_{0.3}Co_{0.75}$ electrodes as a function of the number of cycles. The discharge capacity of the $MmNi_{3.55}Mn_{0.4}Al_{0.3}Co_{0.75}$ alloy reaches a maximum value of 270 mAh/g after 12 cycles, decreases to about 200 mAh/g after 25 cycles and remains constant after that. However, the discharge capacity of the $MmNi_{3.55}Mn_{0.4}Al_{0.3}Fe_{0.75}$compound reaches a maximum value of 200 mAh/g after 9 cycles, decreases to about 180 mAh/g after 25 cycles and then remains constant. The capacity decrease is mainly due to the surface layer oxidation and corrosion phenomena. Pan et al. [14] and Geng et al. [15] assume that the loss in discharge capacity is due to the deterioration of the negative electrode material with increasing the number of charge-discharge cycles. In fact, during the cycling, the rare earth elements, such as La or the transition metal such as Mn segregate, to the grain boundaries, where they were subject to corrosion. The corrosion is disposed on the surface of the grain particles as a needle-shaped $La(OH)_3$ or as Mn_3O_4. This decease may be also attributed to the oxidation of iron on the alloy surface which limits the hydrogen transfer from the surface to the bulk of the alloy and consequently to a loss in the amount of hydrogen stored in the material. The cobalt-containing alloy has a higher capacity and a better stability than the iron-containing alloys. The negative electrode charging efficiency was also improved by the Co additive. With respect to the relative discharge capacities of these alloys, it is easy to conclude that the substitution of the cobalt by iron decreases the stability and the life time cycle.

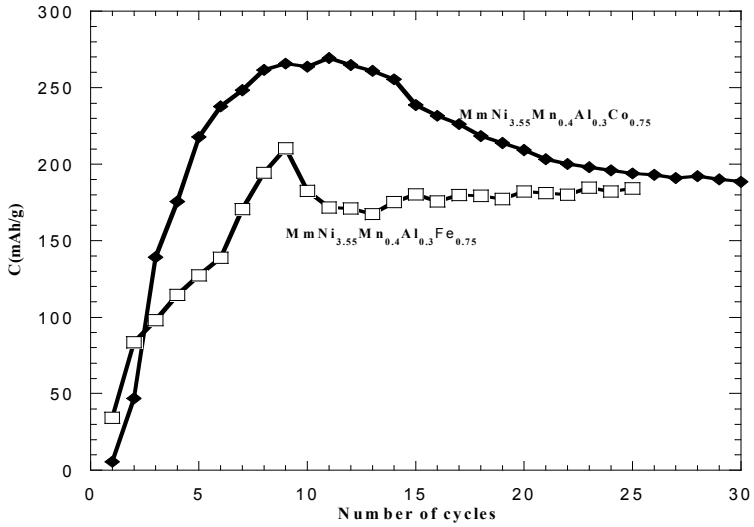

Figure 5. *Variation of the electrochemical discharge capacity of the $MmNi_{3.55}Mn_{0.4}Al_{0.3}Fe_{0.75}$ and $MmNi_{3.55}Mn_{0.4}Al_{0.3}Co_{0.75}$ compounds as a function of the cycle number [24].*

3.3.2. Cyclic Voltammetry

The cyclic voltammogramms of the $MmNi_{3.55}Mn_{0.4}Al_{0.3}Co_{0.75}$ and $MmNi_{3.55}Mn_{0.4}Al_{0.3}Fe_{0.75}$ compounds at different scan rates (10, 20, 30, 40 and 50 μv/s) after activation are illustrated in Fig. 6 and 7, respectively. The observed anodic peak is attributed to the oxidation of the absorbed hydrogen atoms on the surface. These figures show that the anodic current peak increases and its potential slightly shift to the positive direction with increasing the scan rate. Fig. 8 shows that the variation of the anodic peak potential (E_{pic}) of this electrode has a linear dependence on log (v). So, it can be concluded that the electrode formed by these alloys form an irreversible system [16] .In the case, the anodic peak potential can be written by the Equation 1 as [16].

$$\frac{d E_{ap}}{d \log(v)} = \frac{2.3 \; R \; T}{2 \; \alpha \; n \; F} \qquad (1)$$

where v is the scan rate, R is the constant of rare gas, T is the temperature of the electrochemical cell, α is the charge transfer coefficient, n the number of exchanged electron and F the faraday constant. So, this formula allows the determination of the value of the charge transfer coefficient α.

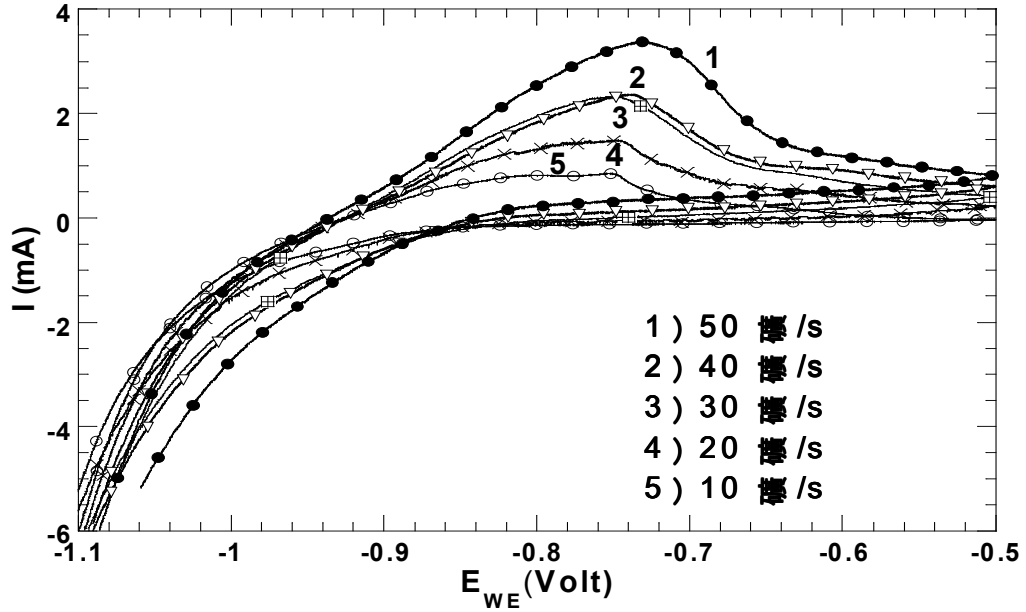

Figure 6. *Cyclic voltammograms of the $MmNi_{3.55}Mn_{0.4}Al_{0.3}Co_{0.75}$ compound obtained at potential scan rates: 10, 20, 30, 40 and 50 μV s^{-1} [24].*

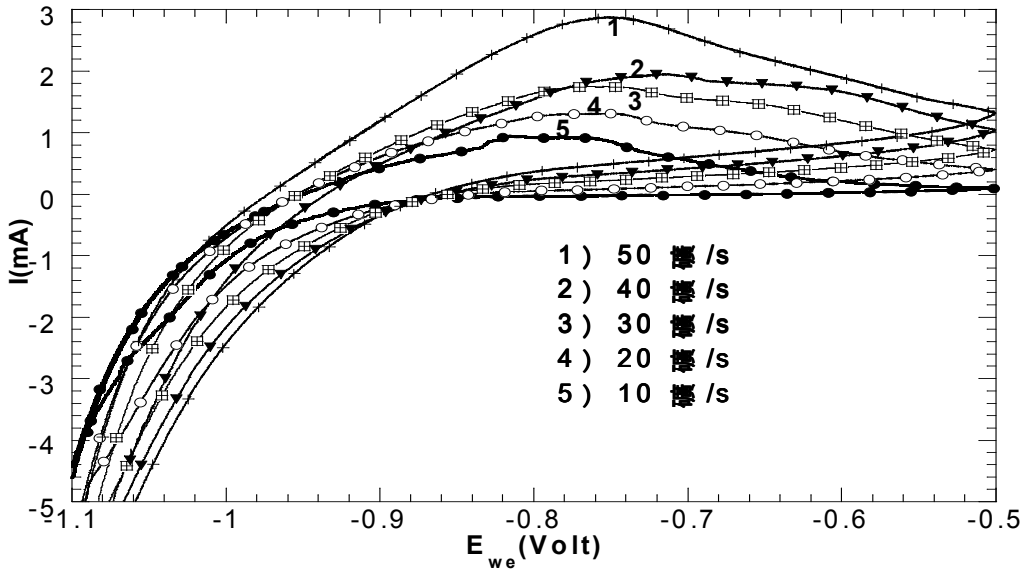

Figure 7. *Cyclic voltammograms of the $MmNi_{3.55}Mn_{0.4}Al_{0.3}Fe_{0.75}$ compound obtained at potential scan rates: 10, 20, 30, 40 and 50 μV s^{-1} [26].*

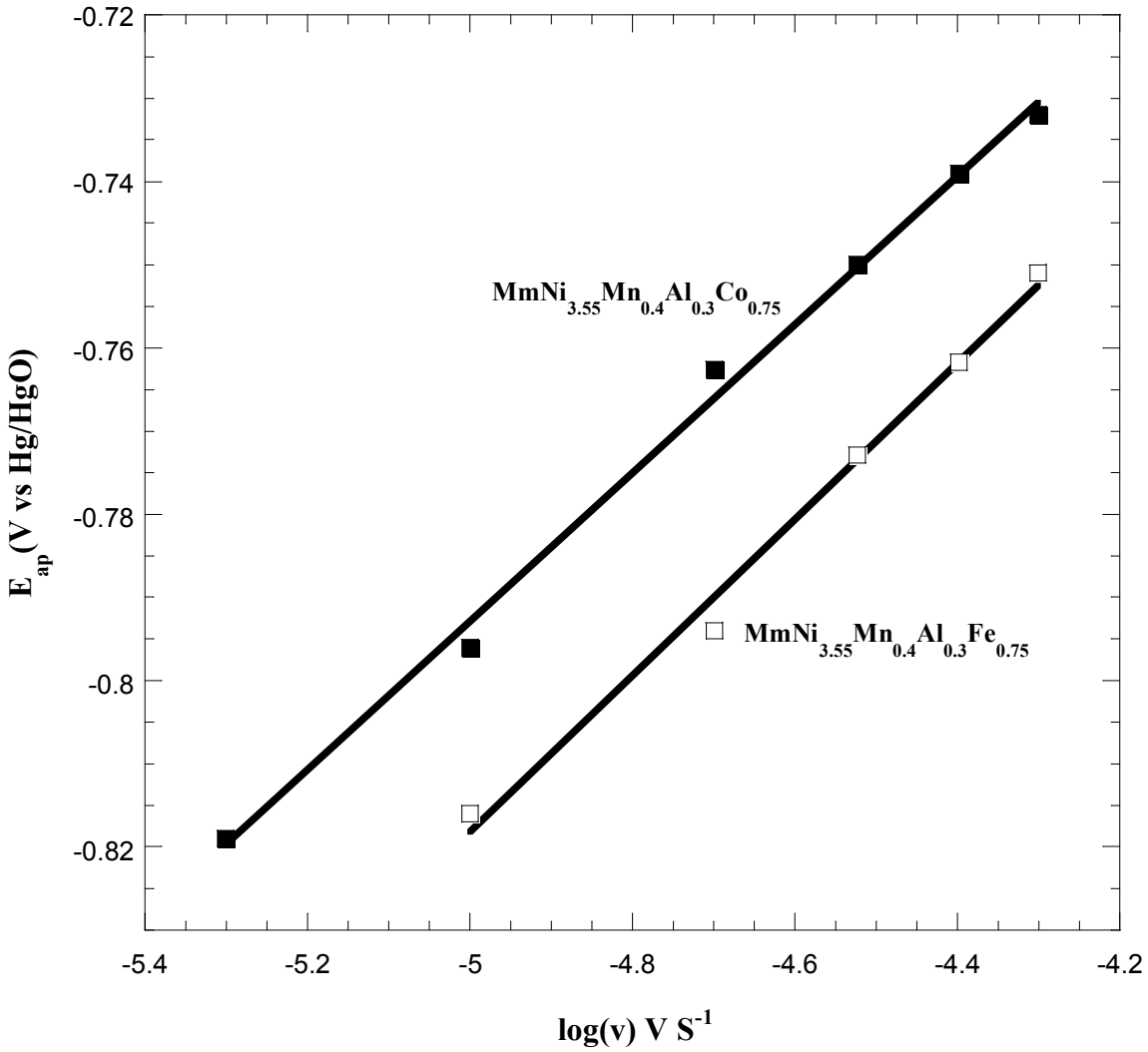

Figure 8. *Variation of the anodic peak potential of cyclic voltammograms of the $MmNi_{3.55}Mn_{0.4}Al_{0.3}Fe_{0.75}$ and $MmNi_{3.55}Mn_{0.4}Al_{0.3}Co_{0.75}$ electrodes as a function of log(v) [24, 26].*

Fig. 9 shows the variation of the anodic peak current versus the square root of the scan rate ($v^{1/2}$) is linear. So, for a semi-infinite diffusion and an irreversible transfer can be expressed by Equation 2 as [16]:

$$I_{ap} = 0.496\ \alpha^{1/2}\ (n\ F)^{3/2}\ S\ C_0\ [\frac{V D}{R T}]^{1/2} \quad (2)$$

Where α is the charge transfer coefficient, n is the number of the exchanged electron, F is the Faraday constant, s is the geometrical surface of the working electrode (cm^2), C_0 is the concentration of the diffusing species (mol cm^{-3}), D is the hydrogen diffusion coefficient ($cm^2\ s^{-1}$) and V is the potential scan rate ($V\ s^{-1}$). The concentration of diffusing species C_0 is determined by Equation 3 as:

$$C_0 = \frac{Q\ M}{m\ F\ V_M} \quad (3)$$

Where, M, m, F and V_M are respectively, the molecular mass, the effective mass of material, the Faraday constant and the molecular volume of material. Q is the amount of the hydrogen anodic oxidation during the anodic seep of cyclic voltammetry [17]. It is expressed by equation 4 as:

$$Q = \int_{t_1}^{t_2} i\,dt = \int_{E_1}^{E_2} \frac{i}{V} dE \quad (4)$$

Where, t_1, t_2 and t are times and E_1, E_2 and E are potentials, i is the anodic current and V is the scan rate. According to Equation 2, the hydrogen diffusion coefficient in this metal hydride electrode can be determined using the slope of the curve $I_{ap} = f(v^{1/2})$.

The values of the charge transfer coefficient α and the hydrogen diffusion coefficient D_H, calculated from the slope of the curve $E_{ap} = f(\log(v))$ and $I_{ap} = f(v^{1/2})$ as explained above, are given in Table 4. The values of the charge transfer coefficient are close to 0.5. This shows symmetry of the reaction of insertion and desinsertion of hydrogen in the bulk of material in terms of reversibility and diffusivity of hydrogen.

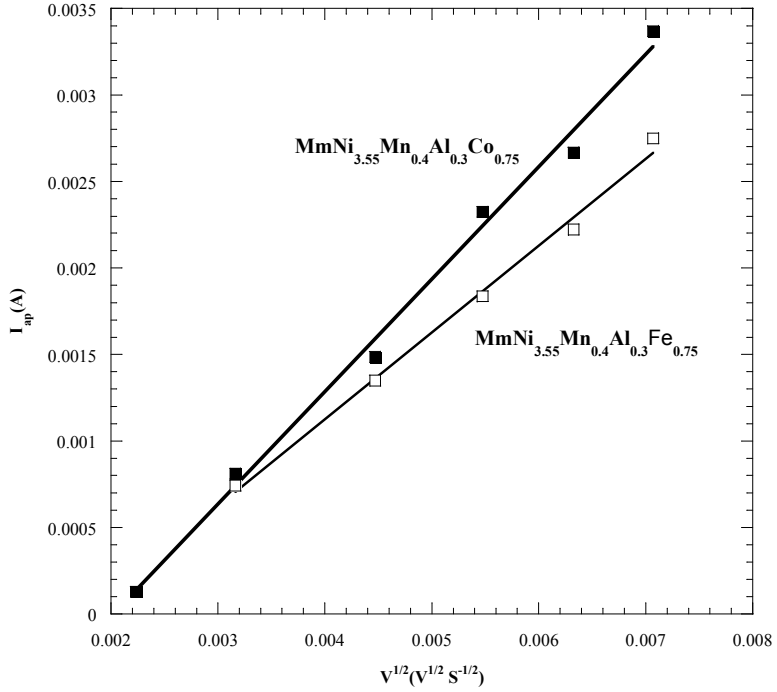

Figure 9. *Variation of the anodic peak current of the cyclic voltammograms of $MmNi_{3.55}Mn_{0.4}Al_{0.3}Fe_{0.75}$ and $MmNi_{3.55}Mn_{0.4}Al_{0.3}Co_{0.75}$ electrodes as a function of the square root of the potential scan rate [24, 26].*

Table 4. *Charge transfer (α) and hydrogen diffusion D_H coefficient of the $MmNi_{3.55}Mn_{0.4}Al_{0.3}Fe_{0.75}$ and $MmNi_{3.55}Mn_{0.4}Al_{0.3}Co_{0.75}$ compounds.*

	charge transfer coefficient α	hydrogen diffusion D_H coefficient $cm^2.s^{-1}$
$MmNi_{3.55}Mn_{0.4}Al_{0.3}Co_{0.75}$ [24]	0.35	$5.86\ 10^{-10}$
$MmNi_{3.55}Mn_{0.4}Al_{0.3}Fe_{0.75}$ [26]	0.4	$3.96\ 10^{-10}$

Based on this table, it can be seen that the value of the hydrogen diffusion coefficient in the Fe-containing alloy is less than that in the Co-containing alloy. The probable reason for this decrease is the reduction of the number of available sites of hydrogen when Co is substituted by Fe. In fact, when the alloy has a higher hydrogen storage capacity and lifetime cycle, it exhibits a good diffusivity of hydrogen. On the other hand, the iron facilitates the oxidation of the surface of the alloy through the combination with oxygen to form an oxide film which in turn inhibits the hydrogen diffusion and leads to a loss in the discharge capacity.

3.3.3. Chronoamperommetry

When we assume that the hydride alloy particles have a spherical form [15-18], the diffusion of hydrogen in the bulk of these particles can be, in the spherical coordinate, given by Eq 5 as:

$$\frac{\partial (r\,c)}{\partial t} = \overline{D}\frac{\partial^2 (r\,c)}{\partial r^2} \qquad (5)$$

Where c is the hydrogen concentration in the alloy, t is time, $\overline{D}$ is the average diffusion coefficient of hydrogen in the bulk and r is a distance from the center of the sphere. Eq 6 gives the solution of the diffusion equation, given by Crank [19] under different boundaries, as:

$$\frac{c-c_0}{c_s-c_0} = 1+\frac{2a}{\pi r}\sum_{n=1}^{\infty}\frac{(-1)^n}{n}\ \mathrm{Sin}\ (\frac{n\pi r}{a})\exp(-\frac{\overline{D}_H}{a^2}n^2\pi^2 t) \qquad (6)$$

Where "a" is the sphere radius and C_0 and C_s are respectively the initial hydrogen concentration in the bulk and the surface hydrogen concentration of the alloy.

Where, F and d are the faraday constant and the density of material respectively.

For a large time, Eq 7 can be rewritten by equation 3 as:

$$\log(i) = \log\left[\frac{6F\overline{D}}{d\,a^2}(C_o - C_s)\right] - \frac{\pi^2\overline{D}}{2.303\,a^2}t \qquad (7)$$

The ± sign in Equation 3 indicates the charge state for the sign (-) and the discharge state for the sign (+). According to Equation 3, $\frac{\overline{D}}{a^2}$ can be evaluated from the slope of the plot of log(i) vs. time "t". Taking into account that the diffusion coefficient of hydrogen $\overline{D}$ is determined by the electrochemical impedance spectroscopy, the radius "a" of the particles, supposed as spherical, concerned by the electrochemical reaction can be calculated from the value of the slope $\frac{\overline{D}}{a^2}$.

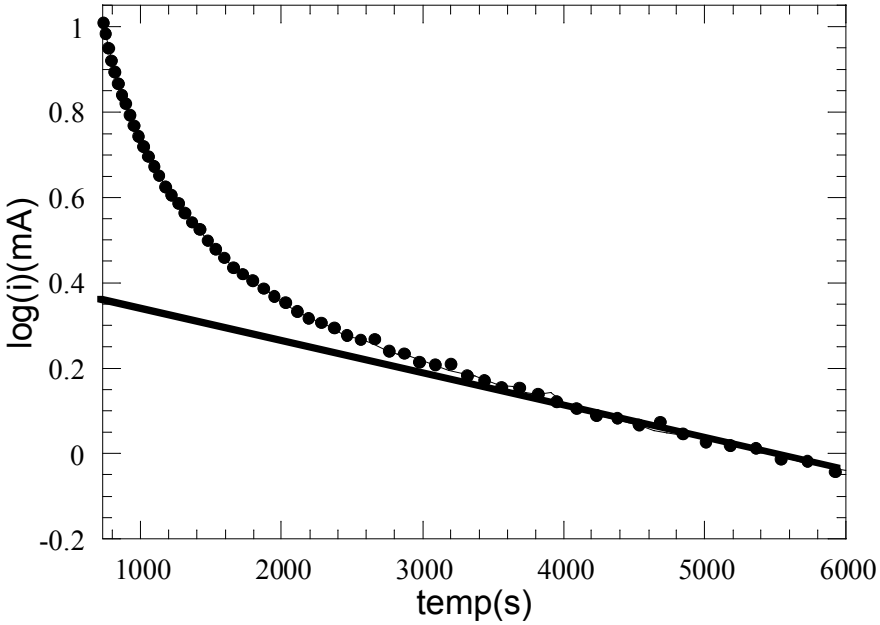

Figure 10. *Variation of the diffusion current of $MmNi_{3.55}Mn_{0.4}Al_{0.3}Co_{0.75}$electrode as a function of time after activation during 13 cycles [24].*

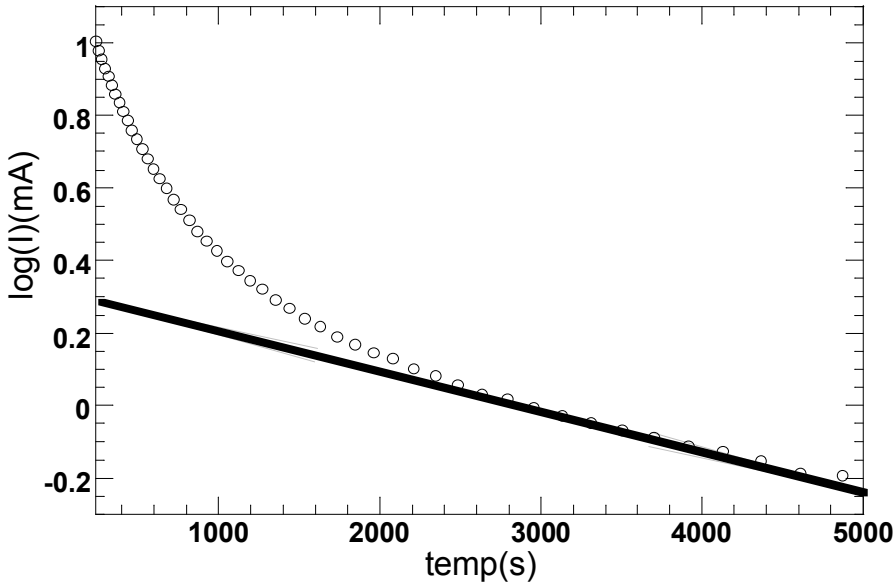

Figure 11. *Variation of the diffusion current of $MmNi_{3.55}Mn_{0.4}Al_{0.3}Fe_{0.75}$electrode as a function of time after activation during 13 cycles [25].*

Fig. 10 and 11, shows that log(i) vs. time "t" may be divided into two time domains. For short time (t < 2000 s), the current decreases rapidly and is under charge-transfer control [9]. At long time (t >2000 s), the diffusion current decreases linearly with time. This reflects that the diffusion current obeys (complies with) equation 3. For the hydrogen diffusion coefficient, $\underline{D}$ is determined by the electrochemical impedance spectroscopy, the variation of the average radius of the particles participating in the electrochemical reaction of the $MmNi_{3.55}Mn_{0.4}Al_{0.3}Co_{0.75}$and $MmNi_{3.55}Mn_{0.4}Al_{0.3}Fe_{0.75}$ alloys of number of cycle are given in table 5, show the average radius decrease of the number of cycles from 100 µm before cycling to 7 µm after 13 cycles. So, we assume that the decrease of the particle size is due to the microcracking of the electrode powder alloys, during the hydrogen absorption and desorption process [14]. Before the charge-discharge process, the alloy ingot were ground mechanically and saved to less than 63 µm in glove box in order to prepare the negative electrode. So, we assume that the decrease of particle size during the cycling and the hydriding is due to the pulverization of powder induced through the expansion of the lattice volume reaching 25 % [14].

Table 5. *The variation of the average radius of the particles participating in the electrochemical reaction of the $MmNi_{3.55}Mn_{0.4}Al_{0.3}Co_{0.75}$ and $MmNi_{3.55}Mn_{0.4}Al_{0.3}Fe_{0.75}$alloys of the number of cycles.*

	a (μm)	
	$MmNi_{3.55}Mn_{0.4}Al_{0.3}Co_{0.75}$	$MmNi_{3.55}Mn_{0.4}Al_{0.3}Fe_{0.75}$ [25]
C_0	105	100
C_1	95	105
C_2	88	104
C_3	80	87
C_5	77	85
C_6	60	82
C_9	33	19
C_{10}	20	14
C_{11}	13	10
C_{12}	11	8
C_{13}	8	7

3.3.4. Impedance Spectroscopy

The kinetic of hydrogen transfer and hydrogen diffusion in the alloys has been investigated using electrochemical impedance spectroscopy. Typical impedance diagrams for the $MmNi_{3.55}Mn_{0.4}Al_{0.3}Co_{0.75}$ and $MmNi_{3.55}Mn_{0.4}Al_{0.3}Fe_{0.75}$electrodes after 13 cyclesof charge-discharge at, respectively, 10 and 100 % state of charge are reported in Fig. 12a and Fig. 13a, respectively. These states of charge correspond to the solid solution α phase (10 %) and the hydride β phase (100 %). All these spectra consist of a very small semicircle in the high frequency (5 KHz to 400 Hz), a slope of about 45° related to the Warburg impedance, in the medium frequency region (300 Hz-100 Hz) and a large semicircle in the low frequency region(100 Hz-1 mHz), which marked dependence on the state of charge. The offset of all the curves corresponds to the electrolyte resistance (R_e~ 0.52 - 0.79 Ω). For these tow alloys, this value is almost constant whatever the state of charge.

Based on the modeling of the kinetics of the metal hydride electrode [9, 20-21], the semicircle at a high frequency is attributed to the charge transfer reation. So, based on this semicircle, we can determine the charge transfer resistance R_{ct}, the double layer capacitance C_{dl} and the exchange current density I_0. The double layer capacitance and the current density are given, respectively, by Eqs. (8) and (9) as:

$$C_{dl} = \frac{1}{2\pi f^* S \mathrm{R_{ct}}} \tag{8}$$

$$I_o = \frac{RT}{F S \mathrm{R_{ct}}} \tag{9}$$

Where $f^*$is the proper frequency, T the working temperature, n the number of exchanged electron, S the geometric area of the electrode, F the Faraday constant and R_{ct} is the charge transfer resistance. The values of these parameters are given in table 6.

The enlarged view of the Warburg region for the $MmNi_{3.55}Mn_{0.4}Al_{0.3}Co_{0.75}$ and $MmNi_{3.55}Mn_{0.4}Al_{0.3}Fe_{0.75}$ electrodes after 13 cycles of charge-discharge at, respectively, 10 and 100 % state of charge are reported in Fig. 12b and Fig. 13b, respectively.

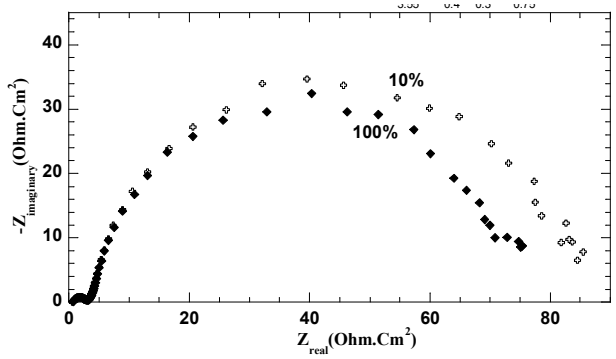

a)

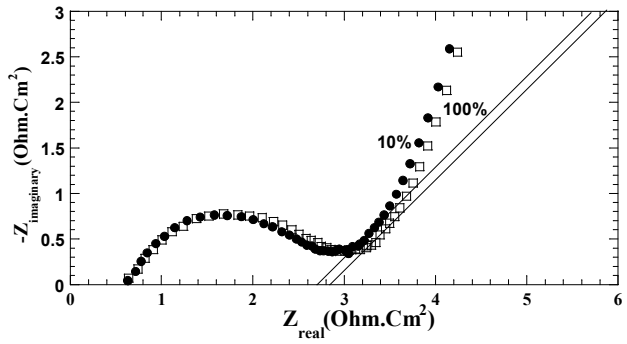

b)

Figure 12. *a) Typical Nyquist plots for the $MmNi_{3.55}Mn_{0.4}Al_{0.3}Co_{0.75}$electrodeat 10 and 100 % state of charge after 13 cycles b) Enlarged view of the Warburg region for $MmNi_{3.55}Mn_{0.4}Al_{0.3}Co_{0.75}$at 10 and 100 % state of charge [24].*

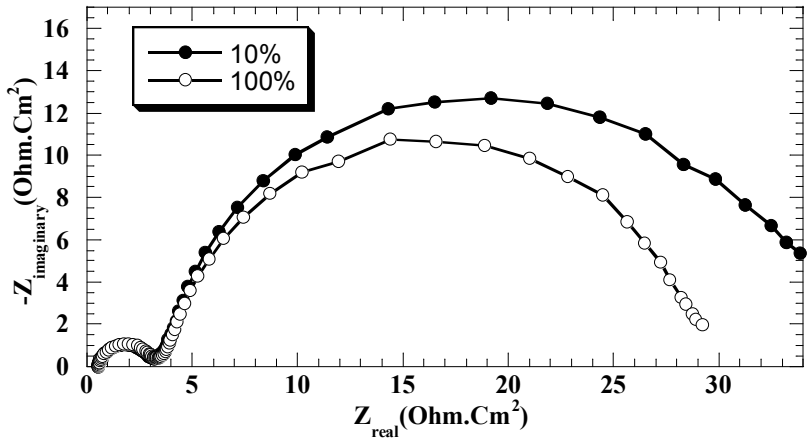

a)

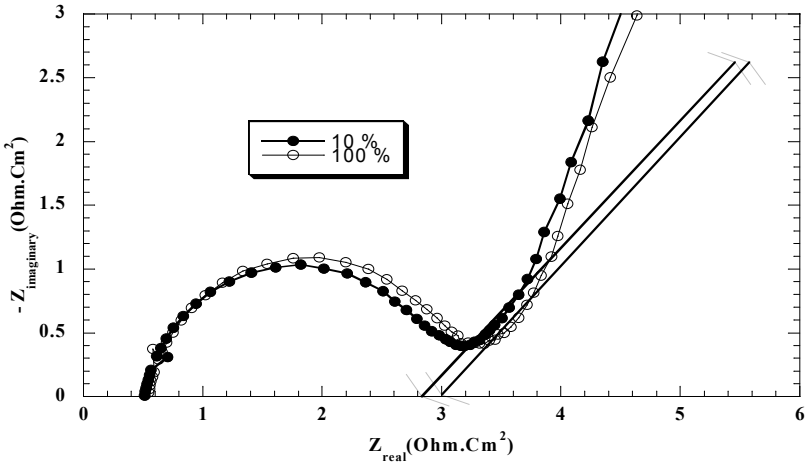

b)

Figure 13. *a) Typical Nyquist plots for the $MmNi_{3.55}Mn_{0.4}Al_{0.3}Fe_{0.75}$electrode at 10 and 100 % state of charge after 13 cycles b) Enlarged view of the Warburg region for $MmNi_{3.55}Mn_{0.4}Al_{0.3}Fe_{0.75}$at 10 and 100 % state of charge.*

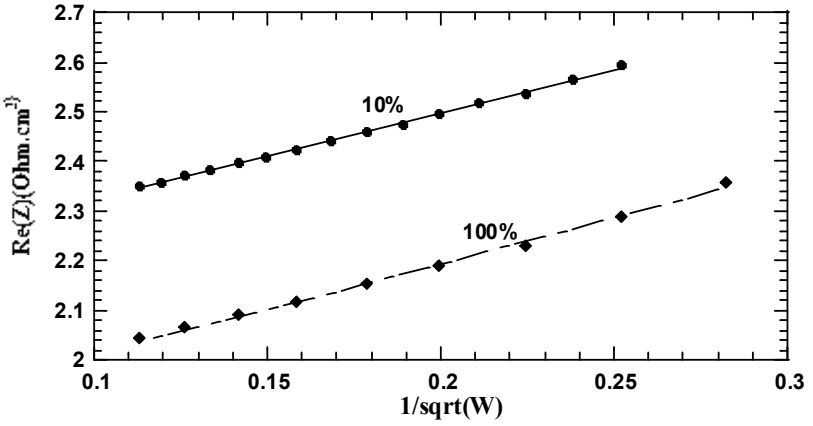

Figure 14. *The variation of Re(Z) versus $W^{-1/2}$ for the of $MmNi_{3.55}Mn_{0.4}Al_{0.3}Co_{0.75}$ compound in the Warburg region at 10 and 100 % state of.*

These figures show that the - Im(Z) has a linear variation versus Re(Z) with an angle of 45^o corresponding to a diffusion process of hydrogen in the bulk material. Fig. 14 shows the variation of Re(Z) versus $W^{-1/2}$, for the of $MmNi_{3.55}Mn_{0.4}Al_{0.3}Co_{0.75}$ compound in the Warburg region at 10 and 100 % state of charge, where W = 2 π f. Under semi-infinite diffusion conditions, the coefficient of the hydrogen diffusion can be calculated from the slope of this plot. In fact, the theoretical slope of this plot is given by Eq. (10) as:

$$A_W = \frac{V_M}{F\,S\sqrt{2\,D_H}}\frac{dE}{dx} \quad (10)$$

Where V_M is the molar volume, dE/dx the slope of the electrochemical discharge isotherm and S is the surface area of the electrode (1 Cm^2). The values of the slope A_W and the hydrogen diffusion coefficient D_H are given in Table 6.

Table 6. *Kinetic parameters of electrodes at 10 et 100 % state of charge after activation.*

	$MmNi_{3.55}Mn_{0.4}Al_{0.3}Co_{0.75}$		$MmNi_{3.55}Mn_{0.4}Al_{0.3}Fe_{0.75}$	
	10 %	**100 %**	**10 %**	**100 %**
$R_e(\Omega)$	0.76	0.79	0.52	0.53
$R_{ct}(\Omega)$	1.65	1.59	2.52	2.74
$C_{dl}(\mu F$	24	20	79	73
$C_{Bf}(mF)$	56	67	109	99
$R_{BF}(\Omega)$	84.07	73.65	34.86	28.47
$I_0(mA)$	15.75	16.35	10.3	9.48
$A_w(\Omega\ S^{-1/2})$	0.353	0.033	0.464	0.0726
$D(cm^2S^{-1})$	$6.64\ 10^{-10}$	$1.6\ 10^{-10}$	$7.27\ 10^{-10}$	$2.51\ 10^{-10}$

For these tow compounds, the hydrogen diffusion coefficient is higher for the α phase and lower for the β phase than the mean value determined by the cyclic voltammetry. We assume that the value of the hydrogen diffusion coefficient depends on the number of interstitial sites susceptible to accept the hydrogen atom. In fact, in the α phase, these sites are more numerous and consequently the hydrogen diffuses easily. EIS measurements indicate that the kinetic properties of the alloy improved with increasing state of charge, mainly due to a fast hydrogen transfer in the bulk of the alloy and the higher electrocatalytic activity of the surface. The transformation of a to ß phase is probably a limiting step in the mechanisms of hydrogenation of metal hydride electrode. So, the D_H is higher. However, in the β phase, the interstitial sites are almost saturated and the hydrogen diffuses hardly [22]. Yuan and Xu [3] and Val∅en et al. [23] indicated that the apparent hydrogen diffusion coefficient depends on the hydrogen content in the alloy in a way that it increases when the state of charge decreases.

4. Conclusion

The aim of this work is to determine the effect of the substitution of the Co by Fe in the $MmNi_{3.55}Mn_{0.4}Al_{0.3}Co_{0.75}$ compound on the thermodynamic and electrochemical properties .The following conclusions could be drawn up:

(1) The values of pressure equilibrium at room temperature of $MmNi_{3.55}Mn_{0.4}Al_{0.3}Co_{0.75}$ and $MmNi_{3.55}Mn_{0.4}Al_{0.3}Fe_{0.75}$ are, respectively, equal to 0.065 and 0.024 bar, which indicates total substitution of cobalt by iron decreases the hydride stability.

(2) The $MmNi_{3.55}Mn_{0.4}Al_{0.3}Fe_{0.75}$ compound exhibits a maximum discharge capacity of 200 mAh g^{-1} after 9 cycles. However, the $MmNi_{3.55}Mn_{0.4}Al_{0.3}Co_{0.75}$ compound exhibits a higher discharge capacity of 270 mAh g^{-1} after 12 cycles. So, the cobalt-containing alloy has a higher capacity and good stability than the iron-containing alloy.

(3) The value of the charge transfer coefficient of the Fe and Co-containing compounds are, respectively, equal to 0.3 and 0.35. This indicates a good electrochemical reversibility reaction for the Fe-containing compounds.

(4) The hydrogen diffusion coefficient D_H values determined by the cyclic voltammetry for the Fe and Co-containing compounds are respectively equal to, $3.96\ 10^{-10}$ $cm^2\ s^{-1}$ and $5.85\ 10^{-10}$ $cm^2\ s^{-1}$.

References

[1] A. Percheron – Guégan, J. C. Achard, J. Sarradin, G. Bronoel, Electrode material based on lanthanum and nickel materials, French patents 75 161 160 (1975), and 7723812 (1977); US patent 688537 (1978).

[2] J. Bouet, B. Knosp, A. Percheron – Guégan, J. M.Cociantelli, Matériau hydratable pour électrode négative d'accumulateur Nickel – hydrure, french patent 92 14662 (1992).

[3] X. Yuan, N. Xu, J. Alloys Comp. 316 (2001) 113-117.

[4] H. Ye, H. Zhang, J. X. Cxheng, T. S. Huang, J. Alloys Comp. 308 (2000) 163-171.

[5] H. Pan, Y. Chen, C. Wang, J. X. Ma, C. P. Chen, Q. D. Wang, Electrochim. Acta 44 (1999) 2263-2269.

[6] J. X. Ma, H. Pan, Y. Zhu, S. Li, C. P. Chen, Q. Wang, Electrochim. Acta 46(2001) 2427-2434.

[7] C. Iwakwra, K. Fukuda, H. Senoh, H. Inoue, M. Matsuoka, Y. Yanamato, Electrochim. Acta 43(14) 2041-2046.

[8] R. Baddour-Hadjem, J. P. Pereira –Ramos, M. Lattroche, A. Percheron-Guégan, ITE Letters on Batteries, New Technologies andMedicine 1(2000) 29-37.

[9] H. Mathouthi, C. Khaldi, M.Ben Moussa, J. Lamloumi, A. Percheron –Guégan, J. Alloys Comp.375 (2004) 297-304.

[10] C. J. Li , X-L. Wang, C-Y-Wang, J. Alloys Comp. 293-295 (1999) 742-746.

[11] T. Sakai, H. Miyamura, N. Kuriyama, H. Ishikawa, I. Uehara, F. Meli, J.Alloys Comp. 238 (1996) 128.

[12] Chuab-Jan Li, Feng-Rong Wang, Wen-Hao Cheng, Wei Li, Wen-Tong Zhoo, J. Alloys Comp. 315 (2001) 218-223.

[13] Y. Zhao, Y. Zhang, G. Wang, X. Dong,S.Guo, X. Wang, J. Alloys Comp. 388 (2005) 284–292.

[14] H. Pan, J. Ma, C. Wang, S. Chen, X. Wan, C. Chen, Q. Wang, J. Alloys Comp. 293 (1999) 648-652.

[15] M. Geng, J. W. Han, F. Feng, O. Derek, N. Wood, J. Electrochem. Soc. 146 (1999) 2371-2375.

[16] A. J. Bard, L. R. Faulkner, Electrochimie: Principes, Methodes et applications, Masson, Paris, (1983).

[17] C. Weixiang, J. Power Sources 90 (2000) 201-205.

[18] G. Zheng, B. N. Popov. R. E. White, J. Electrochem. Soc. 146 (1999) 3639-3643.

[19] J. Cranck, the Mathematics Of Diffusion, 2nd ed., Clarendon press, Oxford, 1975 91.

[20] W. Zhang, M. P. S. Kumar, J. Electrochem. Soc. 142 (1995) 2935-2943.

[21] H. Yang,Y. Zhang, Z. Zhou, J. Wei, G. Wang, D. Song, X. Cao, C. Wang, J. Alloys Comp. 231 (1995) 625-630.

[22] M. Ben Moussa, M. Abdellaoui, H. Mathlouthi, J. Lamloumi, A. PercheronGuégan, J. Alloys Comp. 400 (2005) 239-244.

[23] Lars Ole ValØen, AndrzejLasia, Jens Oluf Jensen, ReidarTunold, Electrochim. Acta 47 (2002) 2871-2884.

[24] M. Ben Moussa, M. Abdellaoui, C. Khaldi, H. Mathlouthi, J. Lamloumi, A. PercheronGuégan, J. Alloys Comp. 399 (2005) 264-269.

[25] M. Ben Moussa, M. Abdellaoui, J. Lamloumi, A. PercheronGuégan, J. Alloys Comp. 575 (2013) 414-418.

[26] M. Ben Moussa, M. Abdellaoui, H. Mathlouthi, J. Lamloumi, A. PercheronGuégan, J. Alloys Comp. 458 (2008) 410-414.